

Predicting Progression of Age-Related Macular Degeneration Using Optical Coherence Tomography and Fundus Photography

Zhichao Wu, BAppSc(Optom), PhD^{1,2}; **Hrvoje Bogunovic**, PhD³; **Rhona Asgari**, MSc³; **Ursula Schmidt-Erfurth**, MD³; **Robyn H. Guymer**, MBBS, PhD^{1,2}

1. Centre for Eye Research Australia, Royal Victorian Eye and Ear Hospital, East Melbourne, Australia
2. Ophthalmology, Department of Surgery, The University of Melbourne, Melbourne, Australia
3. Department of Ophthalmology and Optometry, Christian Doppler Laboratory for Ophthalmic Image Analyses (OPTIMA), Medical University of Vienna, Vienna, Austria

Corresponding Author

Zhichao Wu
Centre for Eye Research Australia
Level 7, 32 Gisborne Street
East Melbourne, VIC 3002, Australia
Email: wu.z@unimelb.edu.au

Financial Disclosure(s):

RHG reports personal fees from Bayer, Novartis, Roche Genentech and Apellis outside the submitted work and research grant from Bayer outside the submitted work. **US-E** is a scientific advisor for Boehringer Ingelheim, Genentech, Heidelberg Engineering, Kodiak, Novartis and Roche outside the submitted work. **ZW**, **HB**, and **RA** report nothing to declare.

Funding Support:

This study was supported by National Health & Medical Research Council of Australia (project grant APP1027624 [RHG] and fellowship grant GNT1103013 [RHG], APP1104985 [ZW]), and BUPA Health Foundation (Australia) (RHG). CERA receives operational infrastructure support from the Victorian Government. The web-based Research Electronic Data Capture (REDCap) application and open-source platform OpenClinica allowed secure electronic data capture. The study is sponsored by the Centre for Eye Research Australia (CERA), an independent medical research institute and a not-for-profit company. The Vienna group received support by the Austrian Federal Ministry of Economy via the Christian Doppler Society.

Running Head: Predicting AMD Progression

Number of Figures: 3

Number of Tables: 1

ABSTRACT

Purpose: To compare the performance of automatically quantified optical coherence tomography (OCT) imaging biomarkers and conventional risk factors manually graded on color fundus photographs (CFP) for predicting progression to late age-related macular degeneration (AMD).

Design: Longitudinal observational study.

Participants: 280 eyes from 140 participants with bilateral large drusen.

Methods: All participants underwent OCT and CFP imaging at baseline and were then reviewed at six-monthly intervals to determine progression to late AMD. CFPs were manually graded and OCT scans underwent automated image analyses to quantify risk factors and imaging biomarkers respectively based on drusen and AMD pigmentary abnormalities. Four predictive models for progression to late AMD or atrophic AMD only were developed (each including age), based on: (1) CFP only (two parameters); (2) OCT biomarkers, minimal (three parameters); (3) OCT biomarkers, extended (seven parameters); (4) CFP and OCT combined (eight parameters).

Main Outcome Measures: Predictive performance for progression to late AMD, examined based on the area under the receiver operating characteristic curve (AUC) for correctly predicting progression.

Results: The AUC for predicting late AMD development was similar for the models based on CFP alone (model 1; 0.80), OCT alone (models 2 and 3; 0.82 for both) and when using both modalities together (model 4; 0.85). In addition, these models also performed similarly for predicting the endpoint of atrophic AMD only (AUC = 0.83, 0.84, 0.85 and 0.88 for models 1, 2, 3 and 4 respectively).

Conclusions: OCT imaging biomarkers could provide an automatic method of risk stratification for progression to vision-threatening late AMD as well as manually grading of CFP.

INTRODUCTION

Age-related macular degeneration (AMD) is a condition where the early hallmarks signs of drusen are typically detected many years before late neovascular or atrophic complications develop. However, AMD progression is highly variable and the ability to accurately identify individuals at high-risk for disease progression remains limited. For example, only approximately one in five eyes that progress over a 5-year period would be correctly predicted based on demographic and clinical AMD severity information at 95% specificity.¹ As such, better methods for risk stratification are needed.

Optical coherence tomography (OCT) is an imaging modality that enables near-cellular and three-dimensional visualization of the retina, which has allowed the detection of disease-related features in AMD that are not visible or difficult to distinguish on clinical examination or color fundus photographs (CFP).²⁻⁴ OCT imaging has also enabled the quantification of drusen volume, internal reflectivity and shape and also the quantity and inner retinal location of hyperreflective foci (HRF). These quantitative OCT imaging biomarkers have previously been reported to be associated with or predict the progression to late AMD,⁵⁻¹¹ and thus show promise as an effective and potentially automated method for risk stratification. Artificial intelligence (AI) based methods were recently developed to detect and quantify morphological changes in standard OCT images, allowing a personalized prediction of disease progression.^{11,12} AI-based analyses, particularly deep learning, offers break-through qualitative and quantitative evaluation of retinal features, particularly in early disease manifestation.¹³ However, no previous studies have yet evaluated the performance of automatically quantified OCT biomarkers compared to conventional methods of risk stratification based on clinical severities manually determined on CFPs.^{14,15} In addition, no studies have examined whether the use of OCT imaging along with conventional CFP clinical severity classifications can further improve the performance of risk stratification.

This study therefore sought to compare the performance of automatically quantified OCT imaging biomarkers against conventional risk factors determined manually on CFPs at predicting the progression to late AMD in a longitudinal cohort of individuals with intermediate AMD and to examine the value of the combined use of both approaches.

METHODS

This study included participants in the sham treatment arm of an interventional study aiming to slow the progression of AMD in those with intermediate AMD, and as such represent the natural history of AMD.¹⁶ Institutional review board approval was obtained at all sites and written informed consent was obtained from all participants. This study was also conducted in accordance with the International Conference on Harmonization Guidelines for Good Clinical Practice and with the tenets of the Declaration of Helsinki.

The primary aim of this study is to determine the predictive performance of automatically quantified OCT imaging biomarkers compared to manually graded risk factors on CFPs at baseline for the development of late AMD in a cohort of intermediate AMD participants, reviewed at six-monthly intervals over a 36-month period. This study only included participants that had at least one follow-up visit.

Participants

This study included individuals at baseline that were at least 50 years of age, had at least one large druse ($>125\ \mu\text{m}$) within $1500\ \mu\text{m}$ of the fovea in both eyes (which meets the definition of intermediate AMD¹⁷), and had a best-corrected visual acuity of 20/40 or better in both eyes. Any participant with late AMD or other ocular, systemic or neurologic disease that could affect retinal assessment were excluded. Late AMD included the presence of neovascular AMD (nAMD; defined as the presence of lesion on fluorescein and indocyanine green angiography, or subretinal hemorrhage associated with fluid on OCT imaging), geographic atrophy (GA) on CFPs (defined as the presence of a sharply delineated, roughly round or oval area of partial or complete retinal pigment epithelium [RPE] depigmentation resulting in improved visibility of the underlying large choroidal vessels $\geq 175\ \mu\text{m}$ in diameter within the central $3000\ \mu\text{m}$ radius region), nascent geographic atrophy (nGA; defined as the presence of subsidence of the outer plexiform layer and inner nuclear layer and/or a hyporeflective wedge-shaped band within Henle's fiber layer^{3,18,19} on OCT imaging) or complete RPE and outer retina atrophy (cRORA; defined as a zone of attenuation or disruption of the RPE band with increased signal transmission below Bruch's membrane $\geq 250\ \mu\text{m}$ in width, associated with overlying photoreceptor degeneration)²⁰.

Imaging and Image Analysis

At each visit, all participants first performed visual acuity measurements, pupillary dilation and then OCT imaging and CFP. Macular-centered, non-stereoscopic digital CFPs were obtained using a site-specific fundus camera with a minimum resolution of 2000×2000 pixels. OCT imaging was performed by obtaining a volume scan covering a $20^\circ \times 20^\circ$ region with 49 horizontal B-scans (25 frames averaged per scan) using the Spectralis HRA+OCT (Heidelberg Engineering; Heidelberg, Germany).

CFPs were manually graded for the presence and size of drusen and presence of AMD pigmentary abnormalities (either hyperpigmentary or hypopigmentary changes) according to the modified Wisconsin grading system by one senior grader.¹⁷ OCT volume scans underwent automated image analysis, including inner retinal layer segmentation using the Iowa Reference Algorithms²¹, and outer retinal layer, drusen and HRF segmentation using deep learning approaches^{22,23} (based on a convolutional neural network previously trained on a different cohort²⁴). The OCT imaging biomarkers quantified and evaluated in this study include cube-root drusen volume, mean and variability of drusen reflectivity, variability of RPE-drusen complex (RPEDC) band height and cube-root volume of HRF overall, and separately for HRF within the outer retinal bands (inner aspect of the ellipsoid zone to outer aspect of the RPE), outer nuclear layer (ONL) and inner retinal layers (above the ONL). These parameters were calculated for the central 5-mm diameter region, and their image segmentation is illustrated in Figure 1.

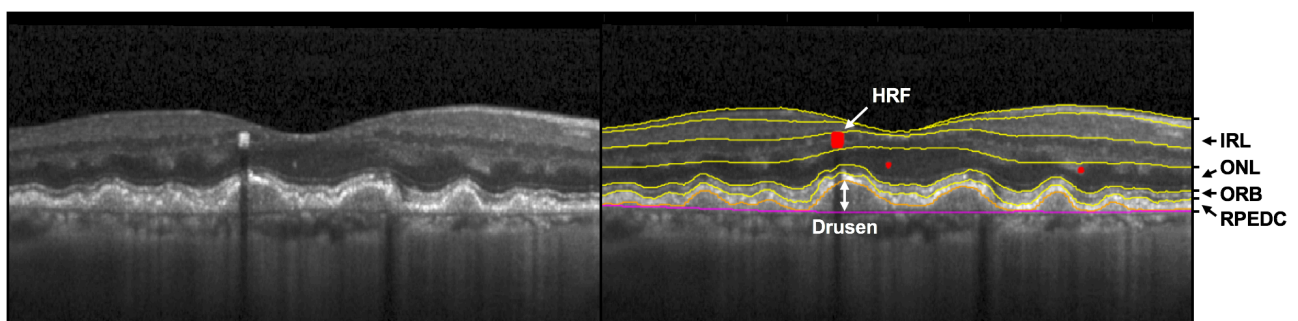


Figure 1: Example of automated image segmentation (original B-scan shown on the left, segmented B-scan shown on the right), which enabled the quantification of hyperreflective foci (HRF; regions highlighted in red), drusen characteristics (region between the orange and magenta

lines) and retinal layers including the retinal pigment epithelium-drusen complex (RPEDC), outer retinal bands (ORB), outer nuclear layer (ONL) and inner retinal bands (IRB).

Predictive Modelling

The endpoints in this study include the development of late AMD or atrophic AMD (defined as the presence of nGA, cRORA or GA). When evaluating the atrophic AMD endpoint, all eyes that developed neovascular AMD were censored at the day of its detection, given that the development of nAMD complicated the assessment of atrophic AMD. Any participant who was lost to follow-up or died during the study were censored at their last visit of assessment, but all other participants were censored at the 36-month visit if they completed the entire follow-up and did not develop an endpoint. Four predictive baseline models for these endpoints were thus developed, each including participant's baseline age as a demographic parameter, as follows:

1. CFP Grading Only (Manual): based on the manually graded presence of pigmentary abnormalities (definitely present vs. questionable or absent). A model with 2 parameters.
2. Minimal OCT Biomarkers (Automated): based on the automatically determined cube-root drusen and HRF volume only. A model with 3 parameters.
3. Extended OCT Biomarkers (Automated): based on the automatically determined cube-root drusen volume, drusen reflectivity parameters, RPEDC band height variability, and cube-root HRF volume in the three separate layers. A model with 7 parameters.
4. CFP Grading (Manual) and Extended OCT Biomarkers (Automated): combining model 1 and 3 above. A model with 8 parameters.

The predictive models were developed using a Cox proportional hazards model for the time to develop the endpoints, using a leave-one-participant-out cross-validation procedure. All parameters were first normalized through subtracting each value by the mean and standard deviation of the values from the derivation cohort (i.e. the whole cohort except for the one participant that was left out). The coefficients (hazard ratios) were used directly to generate a risk score for the one participant left out.

Statistical Analysis

The performance of these models was evaluated using a Wald test of the difference in a covariate-adjusted area under the receiver operating characteristic curve (AUC), when accounting for the maximum follow-up duration (as those with shorter follow-up durations have a lower probability of developing an endpoint) and between-eye correlations within the same participant. The adjusted proportion of variation in the time to develop the endpoints explained by risk scores from each model (R^2) was also calculated to provide an estimate of their predictive ability.²⁵ A bootstrap resampling procedure ($n = 1000$ resamples) was used to calculate standard errors for hypothesis testing for both the AUC and R^2 parameters. All analyses were conducted using STATA software version 14.2 (StataCorp, College Station, TX).

RESULTS:

This study included 280 eyes from 140 participants with a mean age of 70 ± 8 years old (range, 51 to 89 years old) and predominantly (77%) female. Almost all participants completed the 36-month follow-up, except for 6 (4%) participants. A total of 40 (14%) and 8 (3%) eyes developed atrophic and neovascular AMD as their first late AMD endpoints, leading to a total of 48 (17%) eyes that developed late AMD in this study.

At baseline, a total of 82 (29%) eyes were graded as having AMD pigmentary abnormalities on CFP, the median drusen volume was 94.6 nL (interquartile range, 42.9 to 187.5 nL) and median HRF volume was 0.7 nL (interquartile range, 0.4 to 1.4 nL).

Predictive Performance for Late and Atrophic AMD

The predictive performance of the models examined are summarized in Table 1, and it shows that the models using only OCT as imaging biomarkers (model 2 and 3) performed similarly to the one using CFP grading alone (model 1; $P \geq 0.630$). Note that the performance of the models using the minimal compared to extended OCT biomarkers were also similar. The combined use of both CFP and OCT imaging biomarkers (model 4) had the highest predictive performance (AUC = 0.85 and 0.88 for all late and atrophic AMD respectively), but it was also similar to using CFP grading alone

($P \geq 0.049$). Note that the predictive performance for a model using baseline age alone was markedly lower (AUC = 0.56 for both late and atrophic AMD) than the models utilizing the imaging-based AMD risk factors (Models 1 to 4).

Table 1: Predictive performance of the various models based on color fundus photography (CFP) graded and optical coherence tomography (OCT) quantified parameters. All the models included baseline age as a demographic parameter.

Endpoints and Models Evaluated	AUC	95% CI	P-Value*	R ²
Late AMD Endpoint				
Model 1: CFP Grading Only	0.80	0.72 to 0.89	-	0.49
Model 2: Minimal OCT Biomarkers ¹	0.82	0.74 to 0.90	0.710	0.60
Model 3: Extended OCT Biomarkers ²	0.82	0.74 to 0.90	0.640	0.61
Model 4: CFP Grading and Extended OCT Biomarkers	0.85	0.77 to 0.93	0.075	0.72 [#]
Atrophic AMD Endpoint				
Model 1: CFP Grading Only	0.83	0.76 to 0.91	-	0.59
Model 2: Minimal OCT Biomarkers ¹	0.84	0.76 to 0.92	0.870	0.67
Model 3: Extended OCT Biomarkers ²	0.85	0.78 to 0.92	0.630	0.69
Model 4: CFP Grading and Extended OCT Biomarkers	0.88	0.82 to 0.94	0.049	0.80 [#]

Notes: AUC = area under the receiver operating characteristic curve; CI = confidence interval; R² = survival adjusted proportion of variance in time to develop endpoint explained; * = compared to Model 1; ¹ = including cube-root drusen and hyperreflective foci (HRF volume); ² = including cube-root drusen volume, mean and variability of drusen reflectivity, maximum and variability of RPE-drusen complex band height and cube-root volume of HRF separately within the outer retinal bands, outer nuclear layer and inner retinal layers. # = significantly higher at $P < 0.05$ compared to Model 1.

The ROC curves of the predictive performance of the models using manual CFP only and using manual CFP and automated OCT imaging combined are shown in Figure 2.

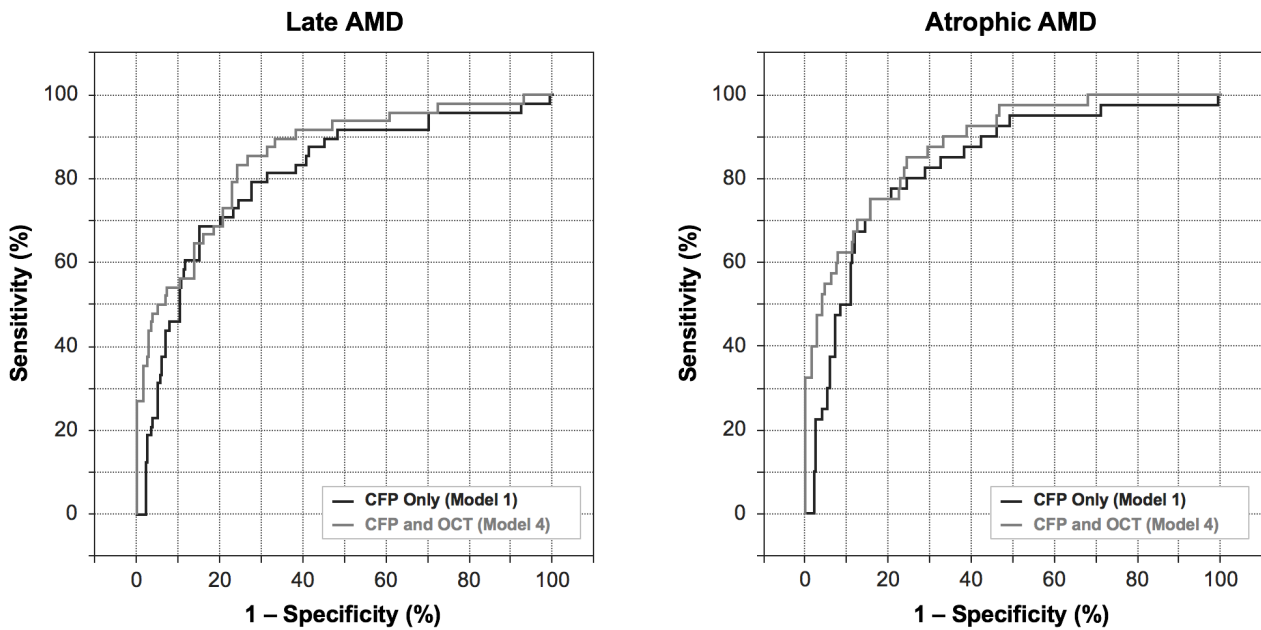


Figure 2: Receiver operating characteristic (ROC) curves of the predictive performance of a model including manually-graded color fundus photograph (CFP) parameters only (black line) compared to a model that also included automatically derived optical coherence tomography (OCT) imaging biomarkers (grey line) for the development of late or atrophic age-related macular degeneration (AMD); note both models included baseline age as a parameter.

The proportion of variance explained in the time to develop endpoints by both models that used OCT biomarkers alone (Models 2 and 3; $R^2 = 0.60$ and 0.61 for late AMD respectively, $R^2 = 0.67$ and 0.69 for atrophic AMD respectively) were not significantly different from that explained by the models using CFP grading alone (Model 1; $R^2 = 0.49$ and 0.59 for late and atrophic AMD respectively; $P \geq 0.150$). However, the model including both CFP and OCT information (Model 4) showed the highest proportion of variance explained ($R^2 = 0.71$ and 0.80 respectively for late and atrophic AMD respectively) and this was significantly better than the model using CFP alone (Model 1; $P \leq 0.010$); these findings are summarized in Table 1. A model using baseline age alone explained almost none of the proportion of the variation in time to develop endpoints ($R^2 = 0.01$ for both late and atrophic AMD).

Examples of Findings in this Study

Four exemplary cases illustrating the findings of this study are shown in Figure 3. In Cases 1 and 2, both Model 1 (using CFP) and 2 (using OCT imaging) showed similar performance for predicting the development of late AMD. In Case 3, the model based on OCT imaging (Model 2) performed better than the model based on CFP (Model 1) for predicting the development of late AMD due to the absence of definite pigmentary abnormalities on CFP. In Case 4, the model based on CFP (Model 1) performed better than the model based on OCT imaging (Model 2), due to the relatively lower drusen and HRF volume on OCT imaging compared to the definite presence of pigmentary abnormalities on CFP.

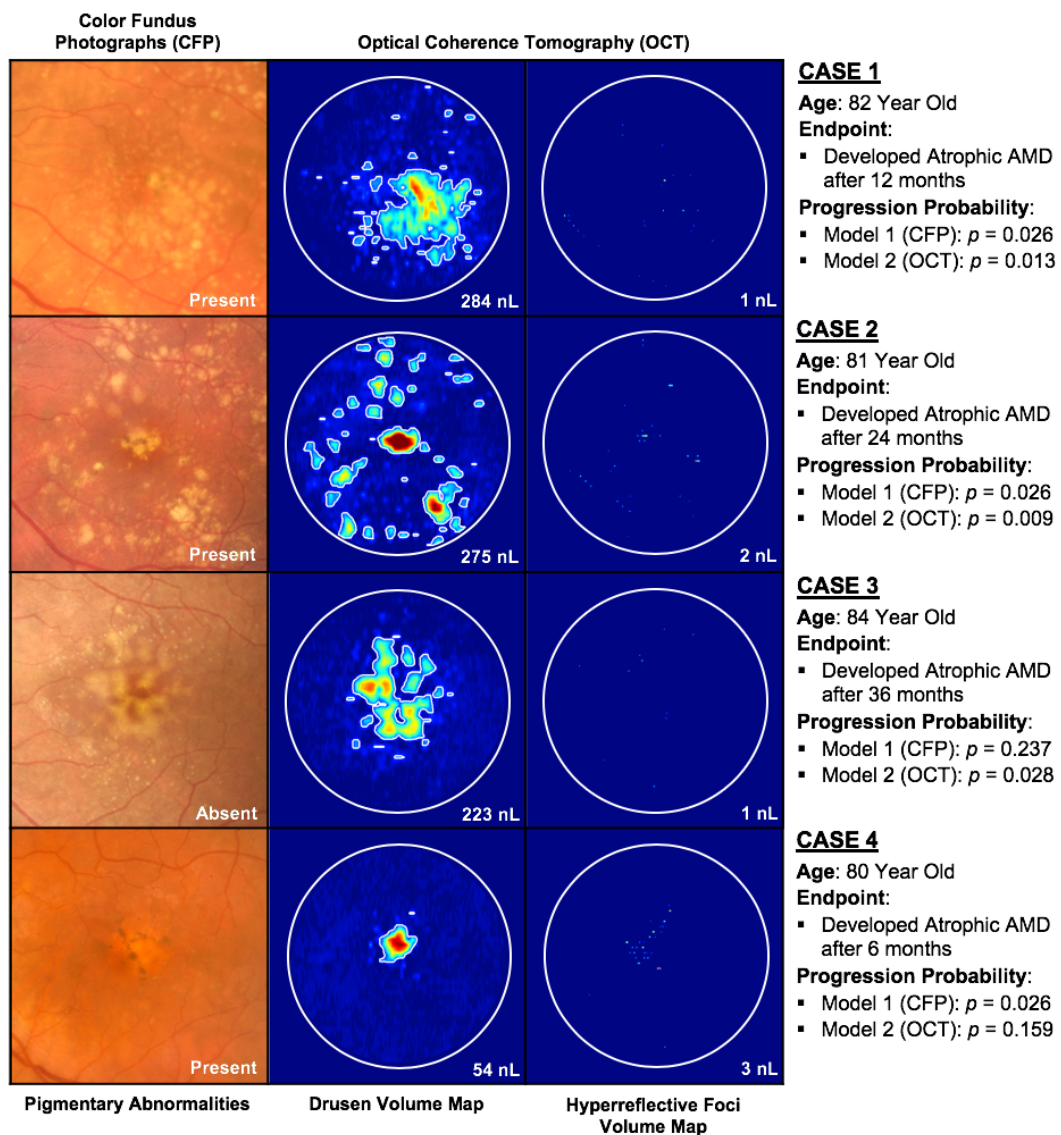


Figure 3: Exemplary cases illustrating the findings of this study, with the presence or absence of pigmentary abnormalities on color fundus photographs (CFP) shown in the first column, drusen

and hyperreflective volume maps on optical coherence tomography (OCT) shown in the second and third columns respectively, and a description of the case on the right of each row. Cases 1 and 2 provide examples where predictive models based on either CFP or OCT imaging parameters (Models 1 and 2 in this study respectively) performed similarly at predicting the development of late age-related macular degeneration (AMD). Case 3 shows an example of an eye where the model based on OCT imaging (Model 2) performed better than the model based on CFP (Model 1), whilst Case 4 shows an example of the opposite case, where the model based on CFP performed better than the model based on OCT imaging.

DISCUSSION

This study demonstrated that automatically quantified OCT imaging biomarkers (relating to drusen and HRF characteristics) performed not significantly different from manually graded parameters on CFP (of drusen and pigmentary abnormalities) in its predictive performance of progression to late AMD in individuals with bilateral large drusen when using data at baseline only (i.e. a single time-point). The combination of the OCT biomarkers and CFP grading explained a larger proportion of the variation in the time to development of late AMD than when using CFP grading alone. These findings highlight the value of OCT imaging biomarkers in the automated risk stratification of progression in the early stages of AMD.

In this study, we directly compared the performance of automatically quantified OCT imaging biomarkers and conventional grading methods of risk stratification based on CFPs for predicting the progression to late AMD. It is promising that the automation of risk prediction is in line with manual grading as this offers potentially enormous benefits for translation into the clinic, especially in relation to clinical trials that currently rely on expensive and time consuming grading of CFP. The similarity of performance may have been expected since, in this specific setting, both approaches consider the same basic risk factors (drusen and RPE hyperpigmentary abnormalities) known to be associated with disease progression in AMD. However, it may also have been reasonable to expect that the method based on automatically derived OCT imaging biomarkers that quantifies the extent of these risk factors with a greater degree of granularity to provide

improved performance for predicting progression, given that previous studies observed that the extent of these risk factors are associated with the risk of disease progression.^{5-11,26}

We also observed in this study that a model based on drusen and HRF volume performed almost as well as a model that included additional factors such as mean and variability of drusen reflectivity, variability of RPEDC height and HRF volume for different intraretinal locations. With the exception of the intraretinal location of HRF (which a previous study observed to be an important risk factor for progression⁶), other previous studies have shown that these additional parameters may not contain substantial prognostic information.^{7,11,28} However, there may be other parameters that have not been evaluated or quantified in this or previous studies that might confer important prognostic information. It should also be noted that the OCT imaging biomarkers summarize image characteristics (e.g. variability of voxel intensity) without consideration of morphological patterns that may confer different prognosis.^{29,30} Such patterns could be better exploited using deep learning approaches, although its performance when compared to a model based on drusen and HRF volume remains to be established.

Nonetheless, the findings of this study suggest that it is possible to automatically perform risk stratification on OCT imaging in a manner that achieves similar performance to senior graders who grade CFPs, saving substantial time and costs associated with performing the latter. Since we observed some degree of improvement in the performance for predicting late AMD development when using both OCT imaging and CFPs, the automatically derived risk scores from OCT imaging could supplement the clinical process of risk stratification performed by fundus examination or visual inspection of CFPs.

The limitations of this study include its sample size and number of endpoints reached, and the predominance of atrophic AMD as the endpoint (83% of all late AMD endpoints). It was thus not possible to develop a sufficiently robust model to predict the development of nAMD, being the outcome currently of greater interest (due to the availability of treatments and the value of their early delivery³¹). The OCT imaging biomarkers evaluated in this study also did not include the presence and/or extent of reticular pseudodrusen (RPD), an important risk factor for individuals with intermediate AMD.³² Furthermore, the predictive models in this study only considered the risk factors at a single timepoint (i.e. baseline). Previous studies have however observed that the

development of late AMD is preceded by the progressive increase in the extent of drusen and HRF,^{6,33-35} and as such, longitudinal measurements of the OCT biomarkers could potentially be used for improved prediction of progression using joint longitudinal survival models or other statistical methods, and warrant investigation in future studies. For such models, the quantitative OCT imaging biomarkers may be advantageous due to the greater granularity in its measurements when compared to manually graded risk factors on CFP that are typically binary (and thus cannot provide information about rate of change in its parameters). Finally, employing machine learning-based predictive models which learn to select and combine the set of biomarkers in a non-linear way^{11,12} are expected to further boost the performance of OCT-based models.

In conclusion, this study showed the automatically quantified OCT imaging biomarkers could predict the progression to late AMD in individuals with bilateral large drusen as accurately as manually graded parameters on CFP, and the combination of these two methods improved the proportion of variation explained for the time to develop late AMD. These findings suggest that these OCT imaging biomarkers could provide a means for automatic risk stratification and could be used to aid clinicians in improving their assessment of the risk of progression to vision threatening late AMD.

REFERENCES

1. Seddon JM, Reynolds R, Yu Y, Rosner B. Validation of a prediction algorithm for progression to advanced macular degeneration subtypes. *JAMA ophthalmology* 2013;131(4):448-55.
2. Leuschen JN, Schuman SG, Winter KP, et al. Spectral-domain optical coherence tomography characteristics of intermediate age-related macular degeneration. *Ophthalmology* 2013;120(1):140-50.
3. Wu Z, Luu CD, Ayton LN, et al. Optical Coherence Tomography Defined Changes Preceding the Development of Drusen-Associated Atrophy in Age-Related Macular Degeneration. *Ophthalmology* 2014;121(12):2415-22.
4. Wu Z, Ayton LN, Luu CD, et al. Reticular Pseudodrusen in Intermediate Age-Related Macular Degeneration: Prevalence, Detection, Clinical, Environmental and Genetic Associations. *Invest Ophthalmol Vis Sci* 2016;57(3):1310-6.
5. Amisshah-Arthur K, Panneerselvam S, Narendran N, Yang Y. Optical coherence tomography changes before the development of choroidal neovascularization in second eyes of patients with bilateral wet macular degeneration. *Eye* 2012;26(3):394-9.
6. Christenbury JG, Folgar FA, O'Connell RV, et al. Progression of Intermediate Age-related Macular Degeneration with Proliferation and Inner Retinal Migration of Hyperreflective Foci. *Ophthalmology* 2013;120(5):1038-45.
7. de Sisternes L, Simon N, Tibshirani R, et al. Quantitative SD-OCT Imaging Biomarkers as Indicators of Age-Related Macular Degeneration Progression. *Invest Ophthalmol Vis Sci* 2014;55(11):7093-103.
8. Nathoo NA, Or C, Young M, et al. Optical Coherence Tomography–Based Measurement of Drusen Load Predicts Development of Advanced Age-Related Macular Degeneration. *Am J Ophthalmol* 2014;158(4):757-61. e1.
9. Abdelfattah NS, Zhang H, Boyer DS, et al. Drusen volume as a predictor of disease progression in patients with late age-related macular degeneration in the fellow eye. *Invest Ophthalmol Vis Sci* 2016;57(4):1839-46.
10. Folgar FA, Yuan EL, Sevilla MB, et al. Drusen volume and retinal pigment epithelium abnormal thinning volume predict 2-year progression of age-related macular degeneration. *Ophthalmology* 2016;123(1):39-50. e1.
11. Schmidt-Erfurth U, Waldstein SM, Klimescha S, et al. Prediction of Individual Disease Conversion in Early AMD Using Artificial Intelligence. *Invest Ophthalmol Vis Sci* 2018;59(8):3199-208.
12. Bogunović H, Montuoro A, Baratsits M, et al. Machine Learning of the Progression of Intermediate Age-Related Macular Degeneration Based on OCT Imaging. *Invest Ophthalmol Vis Sci* 2017;58(6):BIO141-BIO50.
13. Schmidt-Erfurth U, Sadeghipour A, Gerendas BS, et al. Artificial intelligence in retina. *Prog Retin Eye Res* 2018;67:1-29.

14. Ferris F, Davis M, Clemons T, et al. A simplified severity scale for age-related macular degeneration: AREDS Report No. 18. *Arch Ophthalmol* 2005;123(11):1570-4.
15. Ferris III FL, Wilkinson C, Bird A, et al. Clinical Classification of Age-Related Macular Degeneration. *Ophthalmology* 2013;129(4):844-51.
16. Guymer RH, Wu Z, Hodgson LAB, et al. Subthreshold Nanosecond Laser Intervention in Age-Related Macular Degeneration: The LEAD Randomized Controlled Clinical Trial. *Ophthalmology* 2019;126(6):829-38.
17. Klein R, Davis MD, Magli YL, et al. The Wisconsin age-related maculopathy grading system. *Ophthalmology* 1991;98(7):1128-34.
18. Wu Z, Ayton LN, Luu CD, Guymer RH. Microperimetry of Nascent Geographic Atrophy in Age-Related Macular Degeneration. *Invest Ophthalmol Vis Sci* 2015;56(1):115-21.
19. Wu Z, Luu CD, Ayton LN, et al. Fundus Autofluorescence Characteristics of Nascent Geographic Atrophy in Age-Related Macular Degeneration. *Invest Ophthalmol Vis Sci* 2015;56(3):1546-52.
20. Sadda SR, Guymer R, Holz FG, et al. Consensus Definition for Atrophy Associated with Age-Related Macular Degeneration on OCT: Classification of Atrophy Report 3. *Ophthalmology* 2017;125(4):537-48.
21. Li K, Wu X, Chen DZ, Sonka M. Optimal surface segmentation in volumetric images—A graph-theoretic approach. *IEEE transactions on pattern analysis and machine intelligence* 2006;28(1):119.
22. Asgari R, Orlando JI, Waldstein S, et al. Multiclass segmentation as multitask learning for drusen segmentation in retinal optical coherence tomography. *arXiv preprint arXiv:190607679* 2019.
23. Schlegl T, Bogunovic H, Klimescha S, et al. Fully automated segmentation of hyperreflective foci in optical coherence tomography images. *arXiv preprint arXiv:180503278* 2018.
24. Schlegl T, Waldstein SM, Bogunovic H, et al. Fully automated detection and quantification of macular fluid in OCT using deep learning. *Ophthalmology* 2018;125(4):549-58.
25. Royston P. Explained variation for survival models. *Stata journal* 2006;6(1):83-96.
26. Fragiotta S, Rossi T, Cutini A, et al. Predictive factors for development of neovascular age-related macular degeneration: a Spectral-Domain Optical Coherence Tomography Study. *Retina* 2018;38(2):245-52.
27. Folgar FA, Chow JH, Farsiu S, et al. Spatial correlation between hyperpigmentary changes on color fundus photography and hyperreflective foci on SDOCT in intermediate AMD. *Invest Ophthalmol Vis Sci* 2012;53(8):4626-33.
28. Sleiman K, Veerappan M, Winter KP, et al. Optical Coherence Tomography Predictors of Risk for Progression to Non-Neovascular Atrophic Age-Related Macular Degeneration. *Ophthalmology* 2017;124(12):1764-77.

29. Khanifar AA, Koreishi AF, Izatt JA, Toth CA. Drusen ultrastructure imaging with spectral domain optical coherence tomography in age-related macular degeneration. *Ophthalmology* 2008;115(11):1883-90. e1.
30. Veerappan M, El-Hage-Sleiman A-KM, Tai V, et al. Optical Coherence Tomography Reflective Drusen Substructures Predict Progression to Geographic Atrophy in Age-related Macular Degeneration. *Ophthalmology* 2016;123(12):2554-70.
31. Finger RP, Wickremasinghe SS, Baird PN, Guymer RH. Predictors of anti-VEGF treatment response in neovascular age-related macular degeneration. *Surv Ophthalmol* 2014;59(1):1-18.
32. Domalpally A, Agron E, Pak JW, et al. Prevalence, Risk and Genetic Association of Reticular Pseudodrusen in Age-related Macular Degeneration. AREDS2 Report 20. *Ophthalmology* 2019; In Press.
33. Schlanitz FG, Baumann B, Kundi M, et al. Drusen volume development over time and its relevance to the course of age-related macular degeneration. *Br J Ophthalmol* 2017;101(2):198-203.
34. Balaratnasingam C, Yannuzzi LA, Curcio CA, et al. Associations between retinal pigment epithelium and drusen volume changes during the lifecycle of large drusenoid pigment epithelial detachments. *Invest Ophthalmol Vis Sci* 2016;57(13):5479-89.
35. Curcio CA, Zanzottera EC, Ach T, et al. Activated Retinal Pigment Epithelium, an Optical Coherence Tomography Biomarker for Progression in Age-Related Macular Degeneration. *Invest Ophthalmol Vis Sci* 2017;58(6):BIO211-BIO26.